Published OnlineFirst November 17, 2009; DOI: 10.1158/0008-5472.CAN-09-1828

Radioimmunotherapy of Breast Cancer Metastases with α-Particle Emitter ^{225}Ac: Comparing Efficacy with ^{213}Bi and ^{90}Y

Hong Song,[1] Robert F. Hobbs,[1] Ravy Vajravelu,[1] David L. Huso,[2] Caroline Esaias,[1] Christos Apostolidis,[3] Alfred Morgenstern,[3] and George Sgouros[1]

[1]Division of Nuclear Medicine, Russell H. Morgan Department of Radiology and Radiological Science, and [2]Department of Molecular and Comparative Pathobiology, Johns Hopkins University School of Medicine, Baltimore, Maryland and [3]Institute for Transuranium Elements, Karlsruhe, Germany

Abstract

α-Particles are suitable to treat cancer micrometastases because of their short range and very high linear energy transfer. α-Particle emitter ^{213}Bi-based radioimmunotherapy has shown efficacy in a variety of metastatic animal cancer models, such as breast, ovarian, and prostate cancers. Its clinical implementation, however, is challenging due to the limited supply of ^{225}Ac, high technical requirement to prepare radioimmunoconjugate with very short half-life ($T_{1/2}$ = 45.6 min) on site, and prohibitive cost. In this study, we investigated the efficacy of the α-particle emitter ^{225}Ac, parent of ^{213}Bi, in a mouse model of breast cancer metastases. A single administration of ^{225}Ac (400 nCi)–labeled anti-rat HER-2/*neu* monoclonal antibody (7.16.4) completely eradicated breast cancer lung micrometastases in ~67% of HER-2/*neu* transgenic mice and led to long-term survival of these mice for up to 1 year. Treatment with ^{225}Ac-7.16.4 is significantly more effective than ^{213}Bi-7.16.4 (120 μCi; median survival, 61 days; P = 0.001) and ^{90}Y-7.16.4 (120 μCi; median survival, 50 days; P < 0.001) as well as untreated control (median survival, 41 days; P < 0.0001). Dosimetric analysis showed that ^{225}Ac-treated metastases received a total dose of 9.6 Gy, significantly higher than 2.0 Gy from ^{213}Bi and 2.4 Gy from ^{90}Y. Biodistribution studies revealed that ^{225}Ac daughters, ^{221}Fr and ^{213}Bi, accumulated in kidneys and probably contributed to the long-term renal toxicity observed in surviving mice. These data suggest ^{225}Ac-labeled anti–HER-2/*neu* monoclonal antibody could significantly prolong survival in HER-2/*neu*–positive metastatic breast cancer patients. [Cancer Res 2009;69(23):8941–8]

Introduction

Radioimmunotherapy of metastatic cancer using α-particle emitter-labeled monoclonal antibodies (mAb) is promising because α-particles can deliver highly focused energy along their short path length (1). The high-energy α-radiation typically causes complex DNA double-strand breaks that are difficult to repair, thus leading to effective tumor cell kill. Preclinical studies using ^{213}Bi-labeled mAbs have shown substantial efficacy in various tumor models including leukemia (2), prostate cancer (3), ovarian cancer (4), and colon cancer (5). We have also shown that ^{213}Bi-labeled anti–HER-2/*neu* mAb (7.16.4) is effective in prolonging the survival of HER-2/*neu* transgenic mice that if left untreated develop widespread metastases, including bone and liver metastases (6). Clinical trials using ^{213}Bi-labeled anti-CD33 mAb to treat myeloid leukemia have shown feasibility and safety (7, 8). However, the short half-life of ^{213}Bi complicates the preparation of the radioimmunoconjugates for clinical use and demands a large amount of ^{213}Bi activity that is limited by worldwide availability of its parent, ^{225}Ac. As a result, the maximum tolerated dose was not reached in the clinical trial at the largest administered activity of 37 MBq/kg (8).

To overcome the short half-life of ^{213}Bi, McDevitt and colleagues (9) proposed the concept of an *in vivo* ^{225}Ac ($T_{1/2}$ = 10 days) generator that would deliver four α-particles to the target site per decay of ^{225}Ac. This compares to one α from ^{213}Bi, making ^{225}Ac much more potent. Indeed, ^{225}Ac-labeled mAbs have greatly improved the survival in lymphoma and ovarian cancer models (9, 10). More recently, ^{225}Ac-labeled antivascular endothelial cadherin mAb targeting tumor neovasculature has been shown to inhibit tumor growth in a prostate cancer (LNCaP) model especially when it is combined with sequential chemotherapy (11). The *in vivo* generator concept has also been investigated in other α-particle emitters. ^{212}Pb ($T_{1/2}$ = 10.6 h, α-particle-emitting daughter ^{212}Bi) *in vivo* generator (^{212}Pb-trastuzumab) has prolonged survival in a colon cancer xenograft model (12). Dahle and colleagues showed that a single injection of ^{227}Th-rituximab ($T_{1/2}$ = 18.7 days, α-particle-emitting daughters ^{223}Ra, ^{213}Rn, ^{215}Po, and ^{211}Bi) is able to completely eradicate 60% of B-cell lymphoma xenografts (13). Because ^{223}Ra, the first daughter of ^{227}Th, has a 10-day half-life and rapidly localizes to bone, α-particles are mainly delivered from ^{227}Th itself and the studies have shown that subsequent daughters do not lead to toxicity.

Several studies have been published to compare the efficacy of α- and β-radiation directly in metastatic tumor models. Behr and colleagues (14) found that ^{213}Bi is therapeutically more effective than the β-emitter, ^{90}Y, in a metastatic colon cancer model. Few studies, however, directly compared the efficacy of *in vivo* α-particle generators with that of conventional α- and β-particle emitters. In this work, we compare the efficacy of targeted therapy using the ^{225}Ac *in vivo* generator with targeted ^{213}Bi and ^{90}Y in a syngeneic HER-2/*neu* metastatic breast cancer model.

HER-2/*neu* is a tumor cell surface tyrosine kinase associated with aggressive phenotype and poor prognosis (15). Targeting HER-2/*neu* with trastuzumab has shown significant clinical benefit in patients with metastatic breast cancer (16). In this study, we show the efficacy of ^{225}Ac-7.16.4 in targeting rat HER-2/*neu*–positive pulmonary metastases. Rat HER-2/*neu* is also expressed on normal lung tissue in this mouse model as determined by Western blot (17). This allows for evaluating efficacy and toxicity of ^{225}Ac-7.16.4 in a model that closely mimics clinical cases where cross-reactivity of tumor antigen expressed on normal organs is common.

Requests for reprints: George Sgouros, Johns Hopkins University School of Medicine, Cancer Research Building II, Room 4M.61, 1550 Orleans Street, Baltimore, MD 21231. Phone: 410-614-0116; Fax: 413-487-3753; E-mail: gsgouros@jhmi.edu.

doi:10.1158/0008-5472.CAN-09-1828

Published OnlineFirst November 17, 2009; DOI: 10.1158/0008-5472.CAN-09-1828

Materials and Methods

Mice, cell line, and mAbs. *neu*-N transgenic mice, ages 6 to 8 weeks, expressing rat HER-2/*neu* under the mouse mammary tumor virus promoter were obtained from Harlan. All experiments involving the use of mice were conducted with the approval of the Animal Care and Use Committee of The Johns Hopkins University School of Medicine. NT2.5, a rat HER-2/*neu*–expressing mouse mammary tumor cell line, was established from spontaneous mammary tumors (18). The NT2.5 cells are maintained in RPMI containing 20% fetal bovine serum, 0.5% penicillin/streptomycin (Invitrogen), 1% L-glutamine, 1% nonessential amino acids, 1% sodium pyruvate, 0.02% gentamicin, and 0.2% insulin (Sigma) at 37°C in 5% CO_2. 7.16.4, a mouse anti-rat HER-2/*neu* mAb, was purified from the ascites of athymic mice. The hybridoma cell line was kindly provided by Dr. Mark Greene (University of Pennsylvania). Rituximab (IDEC Pharmaceuticals), an anti-human CD20 mAb, was used as a negative control.

Radiolabeling of antibody with ^{213}Bi, ^{90}Y, and ^{225}Ac. 7.16.4 was conjugated to SCN-Chx-A′′-DTPA following published protocol (19). ^{90}Y was purchased from Perkin-Elmer and labeled to 7.16.4-Chx-A′′-DTPA (10 mCi/mg) at 37°C for 30 min in acetate buffer (pH 4.5). ^{225}Ac/^{213}Bi (Institute for Transuranium Elements) generator was constructed and ^{213}Bi was labeled to 7.16.4-Chx-A′′-DTPA (10 mCi/mg) as described previously (6). Both ^{90}Y- and ^{213}Bi-labeled 7.16.4 radioimmunoconjugates were purified by MicroSpin G-25 column (GE BioSciences).

^{225}Ac was purchased from Curative Technologies. ^{225}Ac was labeled to mAb in a two-step reaction following McDevitt and colleagues (20). First, ^{225}Ac (0.15-0.2 mCi in 20-80 μL) was chelated to 1 μL (10 mg/mL) *p*-SCN-Bn-DOTA (Macrocyclics) at 56°C for 1 h. Ascorbic acid (1 μL, 150 mg/mL) was added as a radioprotectant and 2 mol/L sodium acetate (40-60 μL) was added to raise the pH to 6.5. The efficiency of ^{225}Ac chelation to DOTA was determined by Sephadex C-25 column (GE Bioscience). Second, 100 μg mAb (~20 μL, 5 mg/mL) was incubated with *p*-SCN-Bn-DOTA-^{225}Ac at 37°C for 45 min (pH 8.5). ^{225}Ac-labeled mAb was purified with a Centricon centrifuge filter unit (YM-10; Millipore).

The reaction efficiency and purity of the radioimmunoconjugates were determined with instant TLC using silica gel impregnated paper (Gelman Science). Instant TLC paper strips were counted the next day with a γ-counter (LKB Wallac; Perkin-Elmer) to allow ^{225}Ac to reach equilibrium. ^{225}Ac-7.16.4 immunoreactivity was determined by incubating 5 ng ^{225}Ac-7.16.4 with excess antigen binding sites (1×10^7 NT2.5 cells) twice on ice for 30 min each time. Immunoreactivity was calculated as the percentage of ^{225}Ac-7.16.4 bound to the cells. Stability of ^{225}Ac-7.16.4 was measured by incubating ^{225}Ac-7.16.4 in cell culture medium containing 20% fetal bovine serum for 30 days and the fraction of ^{225}Ac chelated to DOTA was measured with Sephadex C-25 column and instant TLC. To determine internalization of 7.16.4, NT2.5 cells (2×10^6/mL) were incubated with ^{111}In-labeled 7.16.4 (1 μg/mL) at 37°C. After 0, 10, 20, 30, 60, 120, 240, 360, and 480 min (two samples for each time point) of incubation, reaction was stopped and NT2.5 cells were washed three times with cold PBS. Cell pellet was then incubated with 1 mL NaCl 150 mmol/L/50 mmol/L glycine (pH 2.0) for 10 min at room temperature and washed twice with PBS. Both pellet and supernatant were collected and counted with γ-counter. The activity fraction of the cell pellet was the fraction of internalized 7.16.4 (10).

Specific cell kill *in vitro* by ^{225}Ac-7.16.4. Specific cell kill *in vitro* was determined by colony formation assay. NT2.5 cells were seeded into 96-well plates at 2.0×10^3 per well. NT2.5 cells were then treated with serially diluted ^{225}Ac-7.16.4 or ^{225}Ac-rituximab (0.2-20 nCi/mL at a specific activity of 0.10 μCi/μg). After incubation for either 3 or 5 days, NT2.5 cells were trypsinized and replated on cell culture Petri dishes for colony growth. Blocking of cell kill by ^{225}Ac-7.16.4 using unconjugated 7.16.4 (50 μg/mL) was also tested.

Biodistribution of ^{225}Ac-, ^{213}Bi-, and ^{111}In-7.16.4. *neu*-N mice (3 per group) bearing s.c. tumors in the mammary fat pad were injected i.v. with 400 nCi ^{225}Ac-7.16.4. At 1, 6, 24, 72, 144, and 288 h after injection, mice were sacrificed and major organs, including blood, heart, lung, liver, spleen, kidney, stomach, intestine, femur, and tumor, were collected. ^{225}Ac in each organ was counted the next day using an energy window of 150 to 500 keV. To determine the distribution of free ^{221}Fr ($T_{1/2}$ = 4.9 min) and ^{213}Bi that was released after ^{225}Ac decay, the organs were counted right away repeatedly for ^{221}Fr or ^{213}Bi using the 190 to 250 and 400 to 480 keV energy window, respectively. An exponential expression was fitted to the decay curves thus obtained. The fitted activity coefficient at time 0 is the activity concentration at the time of sacrifice. Differences in ^{221}Fr and ^{213}Bi activity at the time of sacrifice and the levels from equilibrium of ^{225}Ac reflect clearance or accumulation of free ^{221}Fr and ^{213}Bi. The time activity curves of free ^{213}Bi and ^{221}Fr in each organ were then constructed with free ^{221}Fr and ^{213}Bi activities at multiple sacrifice time points. Injectates with equivalent injected activity were counted as standards for decay correction. In a separate series of animals, the biodistribution of ^{225}Ac-, ^{213}Bi-, and ^{111}In-7.16.4 to lung metastases was also measured and compared. *neu*-N mice (3 per group) were injected with either ^{225}Ac-, ^{213}Bi-, or ^{111}In-labeled 7.16.4 and sacrificed at 0.5, 1.0, 3.0, and 6.0 h after injection; ^{111}In radionuclide was used as a surrogate for ^{90}Y (21). Lung metastases were collected and counted for ^{225}Ac, free ^{221}Fr, and ^{213}Bi.

Efficacy of ^{225}Ac-, ^{213}Bi-, and ^{90}Y-labeled anti-rat HER-2/*neu* mAb to treat lung metastases. The maximum tolerated dose was determined as the highest administered activity that allows 100% survival with no significant body weight loss (>15%). Healthy *neu*-N mice were injected (5 per group) with 100, 200, 400, 500, 600, 700, or 1,000 nCi ^{225}Ac-7.16.4. Mice were weighed twice per week for 90 days. To evaluate the efficacy of radiolabeled mAbs to treat early-stage micrometastases, 3 days after *neu*-N mice were injected with 1×10^5 NT2.5 cells (i.v.), mice were treated i.v. with (*a*) 400 nCi ^{225}Ac-7.16.4 (n = 12); (*b*) 120 μCi ^{213}Bi-7.16.4 (n = 10); (*c*) 120 μCi ^{90}Y-7.16.4 (n = 5); (*d*) 200 nCi ^{225}Ac-7.16.4 (n = 5); (*e*) 200 + 200 nCi ^{225}Ac-7.16.4 (injected 1 week apart; n = 5); (*f*) 100 μg 7.16.4, unlabeled control (n = 5); (*g*) 400 nCi ^{225}Ac-rituximab, nonspecific control (n = 5); and (*h*) untreated control (n = 10). To evaluate the efficacy of treating late-stage lung metastases, at 18 days after tumor cell inoculation, *neu*-N mice were treated with (*a*) 400 nCi ^{225}Ac-7.16.4 (n = 5), (*b*) 120 μCi ^{213}Bi-7.16.4 (n = 5), and (*c*) 120 μCi ^{90}Y-7.16.4 (n = 5). Mice were monitored and weighed three times a week and were euthanized when significant body weight loss (>15%) or breathing difficulties developed. In survival and long-term toxicity studies, animals were followed for up to 1 year.

At time of sacrifice, all major organs were collected for histopathologic examination. The number of visible lung metastases was counted. Lung metastases were snap-frozen in liquid nitrogen and sectioned with a cryotome into 8-μm-thick slices. The section was fixed in acetone and immunostained with 7.16.4 and a biotinylated rat anti-mouse IgG2a antibody (BD Pharmingen). The stain was developed with a Vectastain ABC kit (Vector Lab) according to the manufacturer's instruction.

Dosimetry. Organ and tumor absorbed doses for ^{225}Ac were calculated based on measured biodistribution data (22). Time activity curves in each organ and in s.c. tumors and small lung metastases were measured and integrated over time to obtain the total disintegration of ^{225}Ac, free ^{221}Fr, and ^{213}Bi. ^{213}Po and ^{217}At, with half-lives of 4.2 μs and 32.3 ms, were assumed to decay at the same position as ^{213}Bi or ^{221}Fr. Absorbed doses for three tumor geometries were calculated: s.c. tumor (~1 cm diameter), small lung metastases (300 μm diameter; day 18), and single cells (day 3). In the s.c. tumor calculation, the α-particle and electron energies of ^{225}Ac were assumed completely absorbed within the tumor. Photon doses were not included because they typically account for <1% of the total absorbed dose. Absorbed doses for normal organs and the s.c. tumor were thus calculated as $D_\alpha = \tilde{A} * \Delta_\alpha / M$; $D_e = \tilde{A} * \Delta_e / M$; $D = D_\alpha + D_e$, where D_α, D_e, and D are the α-particle, electron, and summed α and electron absorbed dose, respectively; $\tilde{A}$ is the total number of disintegrations in an organ/tumor; Δ_α and Δ_e are the mean energy emitted per nuclear transition for α-particles and electrons; and M is the weight of the organ/tumor. The total absorbed doses were calculated as the sum of doses from ^{225}Ac at equilibrium and its free daughters. If an organ is accumulating or depleting free daughters, the dose from free daughters is

Published OnlineFirst November 17, 2009; DOI: 10.1158/0008-5472.CAN-09-1828

added or subtracted from the ^{225}Ac doses at equilibrium. Absorbed doses for single tumor cells (day 3) and small lung metastases (day 18) were also calculated and compared for ^{225}Ac-, ^{213}Bi-, and ^{90}Y-7.16.4. ^{213}Bi and In-111 (surrogate for ^{90}Y) biodistribution data for small lung metastases were used for ^{213}Bi and ^{90}Y dosimetry. The absorbed fractions of electron and α-particle emissions in small lung metastases were calculated using Monte Carlo; these calculations accounted for the range of all of the βs and αs (23). Absorbed doses to single cells were obtained using MIRD cellular *S* values (24, 25). In the single-cell calculations, daughter radionuclides resulting from the decay of 7.16.4-conjuagated ^{225}Ac that was tumor-cell bound but not internalized were assumed to diffuse away and not contribute to the target cell absorbed dose. The fraction of internalized ^{225}Ac-7.16.4 was obtained from the internalization assay.

Statistical analysis. Kaplan-Meier survival analysis or statistical comparisons between groups (Student's *t* test) were done with MedCalc (MedCalc Software). For all studies, the level of statistical significance is set at $P < 0.05$.

Results

Radiolabeling, immunoreactivity, and antibody internalization. Both ^{90}Y and ^{213}Bi labeling efficiencies were ~90% and purities reached ~98% after size-exclusion purification. The two-step ^{225}Ac labeling efficiency was 12.0 ± 3.8% (n = 12). After purification, the purity of ^{225}Ac-7.16.4 was 97.0 ± 1.8% (n = 12). The specific activity of ^{225}Ac-7.16.4 was between 0.06 and 0.10 μCi/μg. The immunoreactivity of ^{225}Ac-7.16.4 was 62.4 ± 5.9% (n = 3), worse than that of ^{111}In- or ^{213}Bi-7.16.4 (~80%). After incubation in 20% bovine serum albumin at 37°C for 30 days, purity of ^{225}Ac-7.16.4 became 80.9 ± 8.2% and 65.9 ± 3.9% as measured by Sephadex C-25 column and instant TLC (n = 3), respectively. 7.16.4 internalizes after binding to NT2.5 cells. The internalized ^{111}In-7.16.4 increased from 1.55×10^{-2} μg/10^6 cells (28.2%) at 5 min after binding started to 3.05×10^{-2} μg/10^6 cells (55.5%) at 120 min and plateaued afterwards to 3.25×10^{-2} μg/10^6 cells (59.2%) at 1,440 min.

***In vitro* cell kill.** ^{225}Ac-7.16.4 was very effective in killing rat HER-2/*neu*–expressing NT2.5 cells (Fig. 1*A*). The activity concentration of ^{225}Ac-7.16.4 that can kill 50% of the NT2.5 cells (ED_{50}) was 2.3 and 6.4 nCi/mL for 5- or 3-day incubation, respectively. When 50 μg/mL unlabeled 7.16.4 was used to block ^{225}Ac-7.16.4, the ED_{50} increased to 9.4 nCi/mL (5-day incubation). The ED_{50} for ^{225}Ac-rituximab was 19.0 and 18.8 nCi/mL when it was incubated with NT2.5 cells for 3 or 5 days. In comparison, the ED_{50} for ^{213}Bi-7.16.4 was 940 nCi/mL.

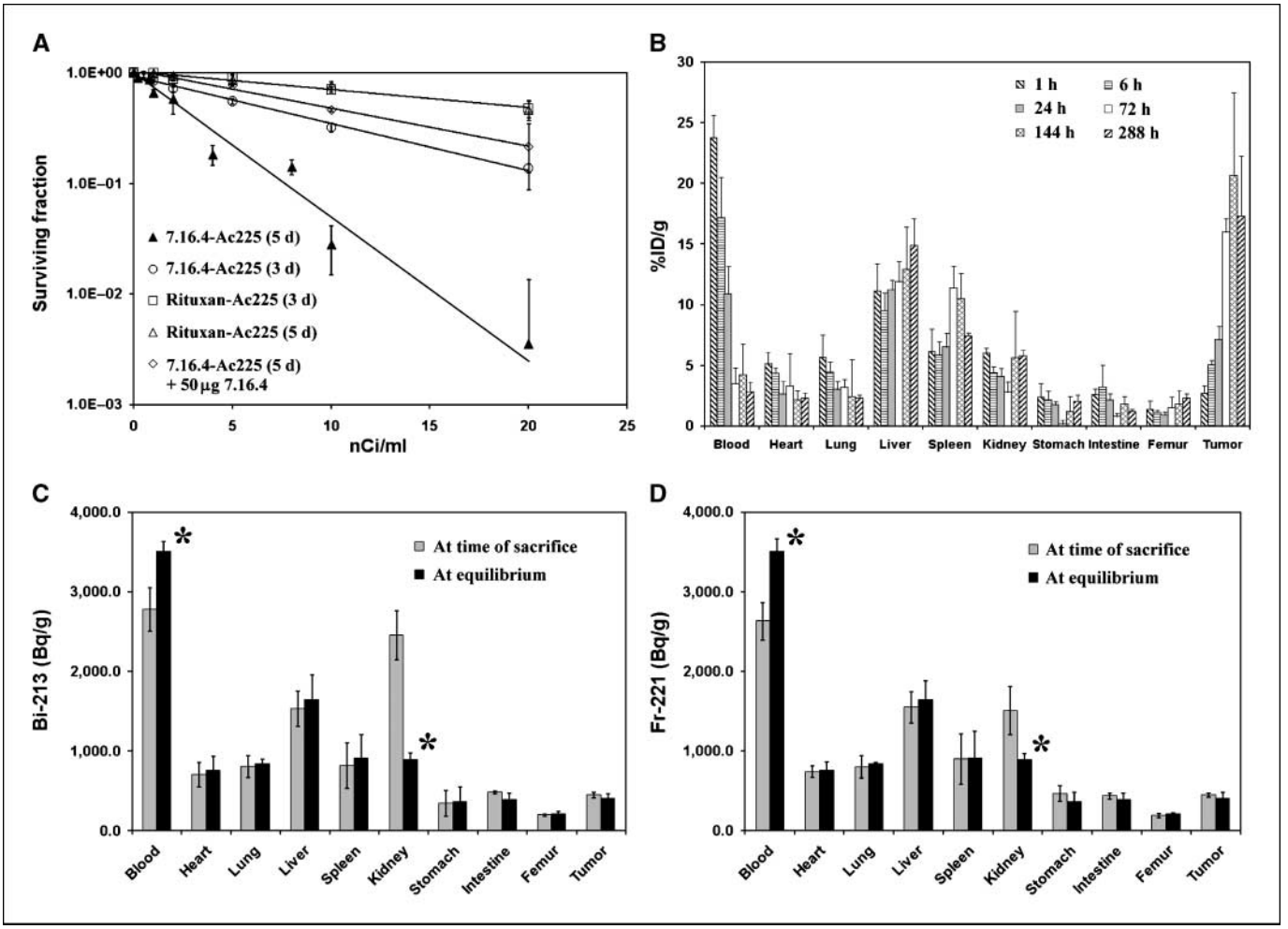

Figure 1. *A, in vitro* kill of NT2.5 breast cancer cells by ^{225}Ac-7.16.4. NT2.5 cells were treated with ^{225}Ac-7.16.4 for 3 d (*open circle*) or 5 d (*closed triangle*) or with the presence of 50 μg/mL unconjugated 7.16.4 (*open diamond*). ^{225}Ac-rituximab was used as nonspecific control to treat NT2.5 cells for 5 d (*open triangle*) or 3 d (*open square*). Survival fraction was calculated by dividing the number of colonies in treatment groups over that in the untreated control group. *B*, biodistribution of ^{225}Ac-7.16.4 in *neu*-N mice at decay equilibrium. Data are expressed as %ID/g ± SD. Biodistributions of free ^{213}Bi (*C*) and ^{221}Fr (*D*) in major organs (at 1 h) are shown at the time of sacrifice and decay equilibrium. *Asterisk,* statistically significant difference. Data are expressed as Bq/g ± SD.

Published OnlineFirst November 17, 2009; DOI: 10.1158/0008-5472.CAN-09-1828

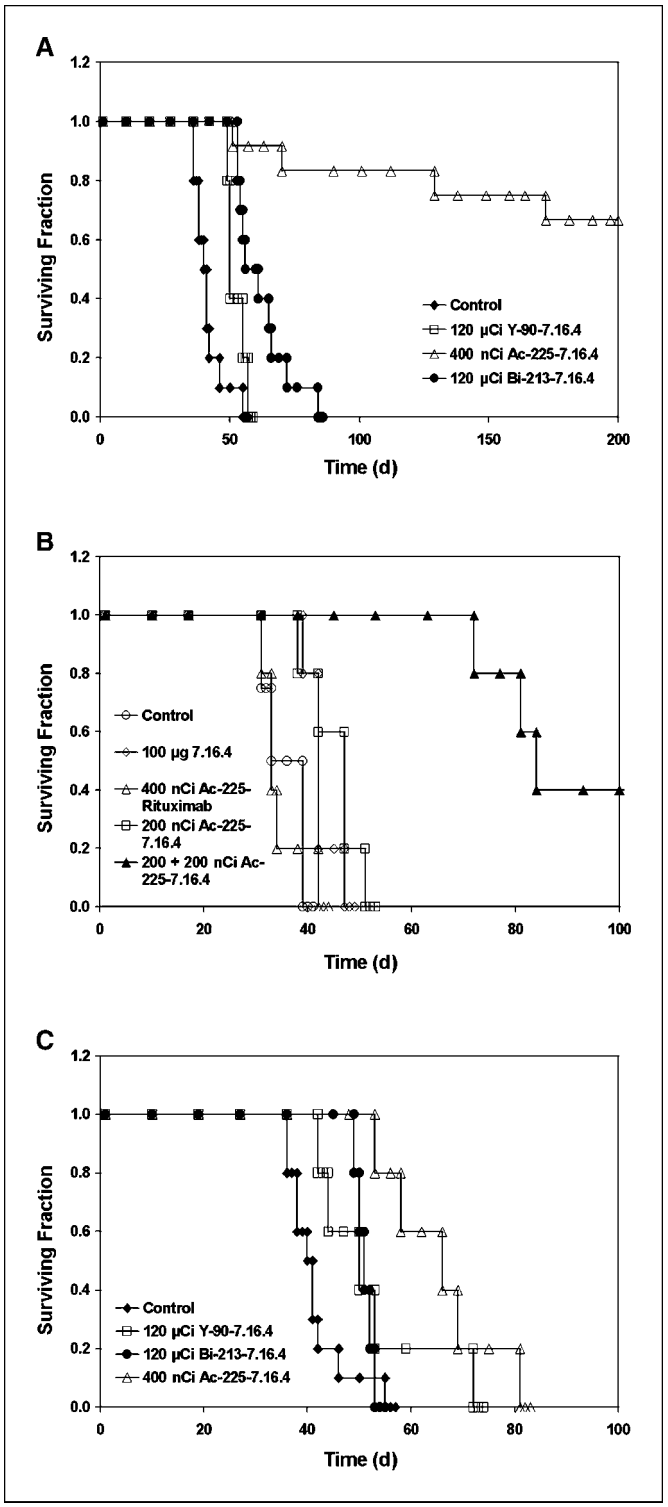

Figure 2. Therapeutic efficacy of ^{225}Ac-, ^{213}Bi-, and ^{90}Y-7.16.4. *A,* Kaplan-Meier survival curves of *neu*-N transgenic mice treated 3 d after i.v. injection of 1×10^5 NT2.5 cells. *neu*-N mice were treated with 400 nCi ^{225}Ac-7.16.4 (*open triangle*; $n = 12$), 120 μCi ^{213}Bi-7.16.4 (*closed circle*; $n = 10$), 120 μCi ^{90}Y-7.16.4 (*open square*; $n = 5$), or untreated (*closed diamond*; $n = 10$). *B, neu*-N mice were treated 3 d after tumor cell inoculation with 100 μg unlabeled 7.16.4 (*open diamond*; $n = 5$), 400 nCi ^{225}Ac-rituximab (*open triangle*; $n = 5$), 200 nCi ^{225}Ac-7.16.4 (*open square*; $n = 5$), 200 + 200 nCi ^{225}Ac-7.16.4 (*closed triangle*; $n = 5$), or untreated (*open circle*; $n = 4$). *C, neu*-N mice were treated 18 d after tumor cell inoculation with 400 nCi ^{225}Ac-7.16.4 (*open triangle*; $n = 5$), 120 μCi ^{213}Bi-7.16.4 (*closed circle*; $n = 5$), 120 μCi ^{90}Y-7.16.4 (*open square*; $n = 5$), or untreated (*closed diamond*; $n = 10$).

Biodistribution of ^{225}Ac-, ^{213}Bi-, and ^{111}In-7.16.4. The biodistribution of ^{225}Ac-7.16.4 at equilibrium in (s.c. mammary fat pad) tumor-bearing *neu*-N mice is shown in Fig. 1*B*. The effective half-life of antibody clearance from blood in the first 72 h was 26.8 h, similar to that of ^{111}In-labeled 7.16.4 (26.3 h). ^{225}Ac-7.16.4 targeting to tumors increased continuously and accumulation peaked at 20.6%/g 6 days after injection. Antibody localization in the tumor was 17.3%ID/g 12 days post-injection. The peak tumor uptake of ^{225}Ac-7.16.4, however, was lower than that of ^{111}In-7.16.4 (~38%ID/g), probably reflecting impaired immunoreactivity of ^{225}Ac-7.16.4.

The biodistributions of free ^{213}Bi and ^{221}Fr at 1 h after ^{225}Ac-7.16.4 injection are shown in Fig. 1*C* and *D*. For ^{213}Bi (Fig. 1*C*), the activity concentration in blood increased from 2,780 Bq/g at time of sacrifice to 3,500 Bq/g at equilibrium ($P = 0.03$), whereas the kidneys activity decreased from 2,450 Bq/g at time of sacrifice to 887.0 Bq/g at equilibrium ($P = 0.005$). Similar pattern was observed for ^{221}Fr (Fig. 1*D*). These data strongly suggest that both free ^{213}Bi and ^{221}Fr cleared from blood through kidneys. The fractions of free ^{213}Bi and ^{221}Fr in blood that ended up in kidneys were 41.1% and 18.7%, suggesting a higher kidney retention rate for ^{213}Bi, which has been attributed to the higher positive charge of ^{213}Bi (Bi^{3+}) that interacts with the negatively charged basement membrane of the glomerulus. In biodistribution study of lung metastases, ^{225}Ac-7.16.4 was found to be 13.7 ± 1.5%ID/g at 144 h, lower than 30.8 ± 1.5%ID/g of ^{213}Bi-7.16.4 at 6 h.

Treating rat HER-2/*neu*–expressing lung metastases with ^{225}Ac-, ^{213}Bi-, and ^{90}Y-7.16.4. The maximum tolerated dose of ^{225}Ac-7.16.4 in *neu*-N mice was found to be 400 nCi in a single injection. Maximum tolerated dose of ^{213}Bi-7.16.4 (120 μCi) and ^{90}Y-7.16.4 (120 μCi) were obtained from literature and confirmed in the *neu*-N model (6, 26). Kaplan-Meier survival curves of *neu*-N mice bearing lung metastases after treatment by radiolabeled anti-rat HER-2/*neu* mAb are shown in Fig. 2*A*. All untreated mice (100%) developed pulmonary metastases, showing signs of labored breath and stress at later stages. Median survival improved to 50 days in ^{90}Y-7.16.4 group ($P = 0.013$) and 61 days in ^{213}Bi-7.16.4 group ($P = 0.0001$) compared with untreated mice (41 days). Eight of 12 mice in ^{225}Ac-7.16.4–treated group achieved long-term (1-year) survival ($P < 0.0001$). Both ^{213}Bi-labeled ($P = 0.025$) and ^{225}Ac-labeled ($P < 0.001$) 7.16.4-treated mice lived significantly longer than the mice treated by ^{90}Y-7.16.4. ^{225}Ac-7.16.4 also improved survival of *neu*-N mice compared with α-emitter ^{213}Bi-7.16.4 ($P = 0.001$). ^{225}Ac-rituximab did not show efficacy in these models with median survivals of only 33 days ($P = 0.99$). Unlabeled 7.16.4 (single i.v. dose 100 μg/mouse) slightly improved median survival to 42 days ($P = 0.014$) and the median survival of *neu*-N mice treated with 200 nCi ^{225}Ac-7.16.4 improved to 47 days ($P = 0.029$). Notably, when a second dose of 200 nCi ^{225}Ac-7.16.4 was administered 1 week after the first 200 nCi injection, median survival improved to 84 days ($P = 0.004$), with 2 of 5 mice achieved long-term survival for up to 1 year (Fig. 2*B*).

To examine the efficacy of ^{225}Ac-7.16.4 on later-stage metastases, *neu*-N mice were treated 18 days after tumor cell injection (Fig. 2*C*), where the average diameter of lung metastases was 296 ± 94 μm ($n = 29$). ^{213}Bi-7.16.4–treated mice have a median survival of 51 days, not a statistically significant improvement over ^{90}Y-7.16.4 with a median survival of 50 days ($P = 0.76$). Although mice treated with ^{213}Bi-7.16.4 at 18 days had a significantly shorter survival compared with those treated at 3 days ($P = 0.0001$), mice treated with ^{90}Y-7.16.4 at 18 and 3 days have about the same median survival of 50 days ($P = 0.96$), suggesting that targeting with the ^{90}Y is less sensitive to the size of the

Published OnlineFirst November 17, 2009; DOI: 10.1158/0008-5472.CAN-09-1828

metastases. The median survival decreased to 66 days for mice treated with ^{225}Ac-7.16.4 at 18 days compared with 3 days (P = 0.0005). Nevertheless, ^{225}Ac-7.16.4–treated mice still survived significantly longer compared with ^{213}Bi-7.16.4 (P = 0.004).

Number of lung metastases. The numbers of visible metastases on the lungs of *neu*-N mice and representative images are shown in Fig. 3. All treated mice have reduced number of lung metastases compared with untreated mice. When treatment was initiated at 3 days, mice treated with ^{213}Bi-7.16.4 and ^{225}Ac-7.16.4 had 8.5 ± 1.8 (P < 0.0001) and 2.9 ± 6.1 (P < 0.0001) lung metastases, significantly less than ^{90}Y-7.16.4–treated mice with 36.7 ± 8.1 metastases. No lung metastases were found in *neu*-N mice surviving ^{225}Ac-7.16.4 treatment (Fig. 3*A, bottom right*). It is also evident that the sizes of the metastases were much larger in ^{213}Bi-7.16.4–treated mice (Fig. 3*A, bottom left*) than those from ^{90}Y-7.16.4–treated mice (Fig. 3*A, top right*), which suggests that ^{213}Bi-7.16.4 is able to eliminate more metastases-initiating cells compared with ^{90}Y-7.16.4 and it takes longer for the surviving tumor cells to grow to a lethal tumor burden. When treatment was initiated at 18 days, the number of metastases found on ^{90}Y-7.16.4–treated mice (32.8 ± 13.2) was similar to that obtained for mice treated with ^{90}Y-7.16.4 at 3 days. More metastases (34.0 ± 13.5) were found on mice treated with ^{213}Bi-7.16.4 at 18 days compared with 3 days (P < 0.0001), indicating reduced efficacy of ^{213}Bi to treat later-stage metastases. ^{225}Ac-7.16.4–treated mice again presented with the fewest number of lung metastases (11.5 ± 3.5) compared with the other two radioisotopes (Fig. 3*B*).

Histopathology and immunohistostaining of rat HER-2/*neu*. Immunohistostaining showed that the HER-2/*neu* expression level decreased on the metastases surviving the treatment of ^{90}Y-7.16.4 (Fig. 4*A, middle*) and ^{213}Bi-7.16.4 (Fig. 4*A, right*) compared with untreated tumors (Fig. 4*A, left*). At 1 year after treatment, no residual tumor cells were found on the lungs of mice treated with 400 nCi ^{225}Ac-7.16.4 (Fig. 4*B, left*) and a single metastatic tumor nodule was found on one of the lungs from a mouse treated with 200 + 200 nCi ^{225}Ac-7.16.4 (Fig. 4*B, right*). No damage to the normal lung tissue was observed in groups treated with ^{225}Ac-7.16.4. Examination of kidneys from these mice, however, revealed shrunken and pale kidneys (Fig. 4*C, left*). H&E staining showed widespread loss of tubular epithelium in the kidney cortex (Fig. 4*C, middle*). In the medulla, there is extensive loss of tubules and replacement with marked fibrosis and a mixed inflammatory infiltrate composed mainly of mononuclear cells and lesser numbers of neutrophils. Scattered dilated cystic structures are visible throughout the cortex and medulla. These observations are also present but less evident in kidneys treated with 200 + 200 nCi ^{225}Ac-7.16.4 (Fig. 4*C, right*).

Dosimetry. The absorbed doses to major organs and tumors are shown in Table 1. Reductions or increases in the absorbed dose from ^{225}Ac at equilibrium with its free daughters are indicated by negative or positive dose contributions. The dose calculations show that free ^{221}Fr and ^{213}Bi are cleared from the blood, lungs, liver, and spleen, whereas kidney, stomach, and intestine are accumulating these daughters. A 400 nCi administration of ^{225}Ac-7.16.4 gives a tumor absorbed dose of 10.49 Gy; no significant depletion or accumulation of free daughters is observed. Absorbed doses of ^{225}Ac-, ^{213}Bi-, and ^{90}Y-7.16.4 to single tumor cells and small lung metastases (~300 μm in diameter) are shown in Table 2. The ^{225}Ac absorbed dose to small metastases is 9.6 Gy, much higher than that of 2.0 Gy from ^{213}Bi and 2.4 Gy from ^{90}Y. Similarly, the 25.3 Gy ^{225}Ac dose to single tumor cells is also higher than that of ^{213}Bi at 2.6 Gy and ^{90}Y at 0.6 Gy. When no antibody-receptor internalization or 100% internalization was considered, ^{225}Ac dose to single cells became 12.0 or 38.6 Gy, respectively.

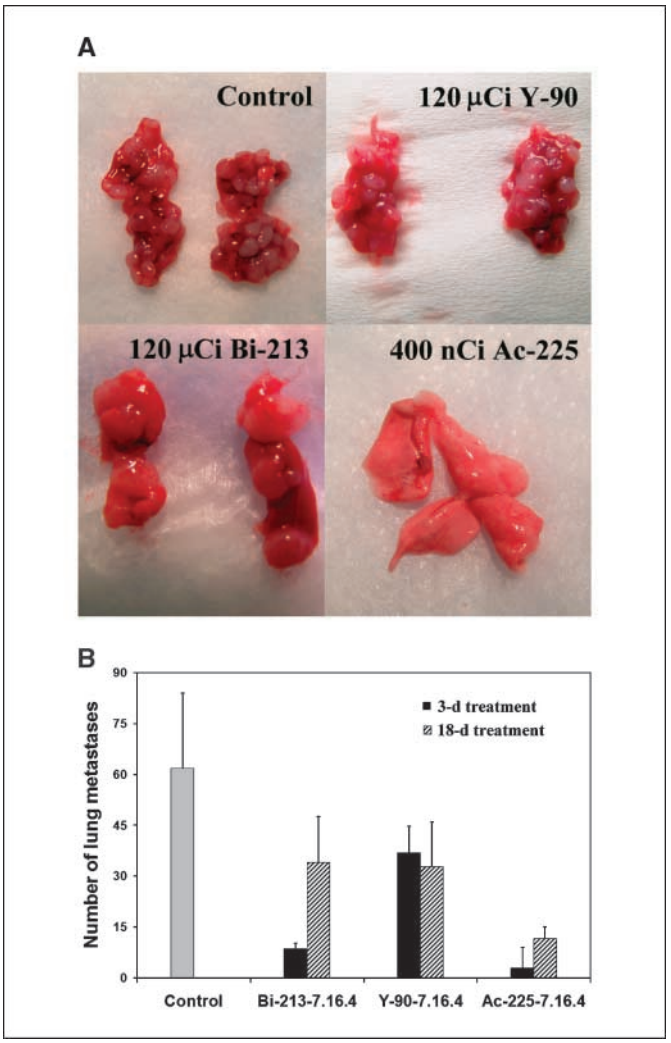

Figure 3. *A,* representative photographs show lungs bearing metastases from *neu*-N mice after treatment by ^{225}Ac-, ^{213}Bi-, and ^{90}Y-7.16.4. These mice were treated at 3 d after tumor cell injection with untreated (*top left*), 120 μCi ^{90}Y-7.16.4 (*top right*), 120 μCi ^{213}Bi-7.16.4 (*bottom left*), or 400 nCi ^{225}Ac-7.16.4 (*bottom right*). *B,* number of lung metastases from mice treated at 3 d (*filled column*) or 18 d (*striped column*) after tumor cell inoculation was counted. Data are presented as average ± SD number of metastases.

Discussion

We showed that α-particle emitter ^{225}Ac-labeled anti-rat HER-2/*neu* mAb is effective in eliminating breast cancer lung metastases, leading to long-term animal survival but also renal toxicity most likely caused by the free daughters of ^{225}Ac (27).

The improved efficacy of α-emitter ^{225}Ac over ^{213}Bi and ^{90}Y can partially be attributed to the higher radiation doses that micrometastases receive from ^{225}Ac. ^{225}Ac emits four α-particles along its decay chain and deposits a total energy of 4.50×10^{-12} J/Bq s, 3.2 and 30.0 times higher than that by ^{213}Bi and ^{90}Y. Furthermore, the majority of α-radiation will be absorbed locally, whereas most of the β-particle energy from ^{90}Y will be deposited outside of micrometastases. An important finding from the biodistribution studies

Published OnlineFirst November 17, 2009; DOI: 10.1158/0008-5472.CAN-09-1828

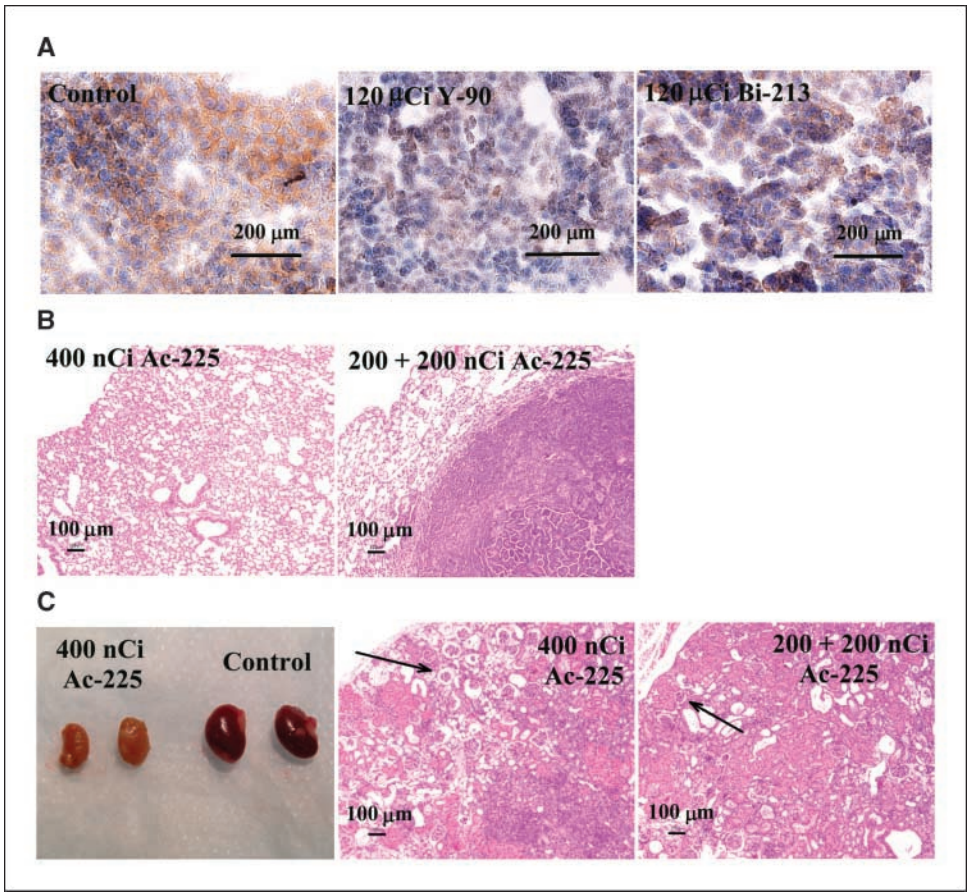

Figure 4. *A,* immunohistostaining of rat HER-2/*neu* expression on lung metastases. *Left,* untreated control; *middle,* treated with 120 μCi ^{90}Y-7.16.4; *right,* treated with 120 μCi ^{213}Bi-7.16.4. *B,* H&E staining of lungs from mice treated with 400 nCi ^{225}Ac-7.16.4 that showed no sign of tumor cells or lung tissue damage (*left*) and of a single metastasis found on the lungs of a mouse treated with 200 + 200 nCi ^{225}Ac-7.16.4 (*right*). *C, left,* representative photographs of kidneys from a *neu*-N mouse surviving 1 y after treatment with 400 nCi ^{225}Ac-7.16.4 (*left pair*) and a healthy *neu*-N mouse (*right pair*). H&E staining of kidneys from *neu*-N mice surviving 1 y after treatment with 400 nCi (*middle*) or 200 + 200 nCi ^{225}Ac-7.16.4 (*right*). *Arrows,* collapse of cortical tissue due to loss of tubular epithelium in the kidney cortex. *Bar,* 100 μm.

is that only a small fraction of ^{221}Fr and ^{213}Bi was released from major organs/tumors, suggesting that these daughters are either retained in the cells due to antibody internalization or there is simply not enough time for a substantial fraction of the daughters to diffuse out of the organs/tumors. The long half-life of ^{225}Ac also helps to deliver more doses to the lung metastases than ^{213}Bi. The biodistribution studies showed that antibody localization to s.c. tumors peaked at least 24 h after injection. For lung metastases, antibody localization is much faster, reaching peak at ~6 h after injection. Nevertheless, for ^{213}Bi, a substantial fraction (>90%) of the decays will have already occurred, greatly reducing the number of α-particles that can be delivered.

The higher potency and longer half-life of ^{225}Ac overcame the ~35% lower immunoreactivity of ^{225}Ac-7.16.4 compared with ^{213}Bi-7.16.4. The immunoreactivity of ^{225}Ac-labeled mAbs seems to vary significantly among different antibodies (20) independent

Table 1. Absorbed doses (Gy) from ^{225}Ac (400 nCi) and its free daughters ^{213}Bi and ^{221}Fr

Organs	^{225}Ac at equilibrium*	Free ^{213}Bi†	Free ^{221}Fr‡	Total α dose§	Total β dose§
Blood	2.71	−0.12	−0.25	2.29	0.05
Heart	1.07	0.00	0.00	1.04	0.02
Lung	0.43	−0.01	−0.01	0.39	0.01
Liver	8.25	−0.01	−0.05	8.00	0.19
Spleen	7.42	−0.01	0.00	7.24	0.17
Kidney	1.20	0.54	0.23	1.91	0.07
Stomach	0.17	0.00	0.04	0.20	0.00
Intestine	0.52	0.00	0.01	0.52	0.01
Femur	0.56	0.00	0.00	0.54	0.01
Tumor	10.49	0.00	0.00	10.24	0.25

*Includes doses from alphas and electrons of ^{225}Ac and daughters in equilibrium.
†Includes doses from alphas and electrons of ^{213}Bi daughters, ^{213}Po, ^{209}Tl, and ^{209}Pb.
‡Includes alphas from ^{221}Fr daughter, ^{217}At.
§Total doses are presented as doses from α- and β-particle emissions, respectively.

Published OnlineFirst November 17, 2009; DOI: 10.1158/0008-5472.CAN-09-1828

Table 2. Absorbed doses to lung metastases or single tumor cells from ^{90}Y-, ^{213}Bi-, and ^{225}Ac-7.16.4

	Lung metastases (Gy)*	Single tumor cells (Gy)†
^{90}Y-7.16.4	2.4	0.6
^{213}Bi-7.16.4	2.0	2.6
^{225}Ac-7.16.4	9.6	25.3
^{225}Ac-7.16.4, 0% internalized	—	12.0
^{225}Ac-7.16.4, 100% internalized	—	38.6

*Electron doses are calculated with a sphere of 300 μm in diameter. All α energy is assumed to be deposited within the sphere. Cross-fire doses are not included.

†Absorbed dose to single cells are calculated with 59.2% internalization fraction and specific activities of 0.1, 10, and 10 μCi/μg for ^{225}Ac, ^{213}Bi, and ^{90}Y, respectively.

of the labeling procedure. When the incubation time in the second step of the reaction was reduced to 30 or 15 min, the immunoreactivity of ^{225}Ac-7.16.4 did not improve in the biodistribution study, with a 16.2%ID/g and 15.4%ID/g tumor localization at 72 h after injection (3 mice per group). Furthermore, stability assay suggested slow but significant release of ^{225}Ac from the antibody, which could also contribute to the lower tumor localization. More studies are needed to understand and improve the immunoreactivity and stability of ^{225}Ac-7.16.4.

The main concern of radioimmunotherapy with α-emitter ^{225}Ac-7.16.4 is the long-term renal toxicity caused by free ^{221}Fr and ^{213}Bi (27). Furosemide or chlorothiazide and competitive metal blockade were found to be effective in reducing renal uptake of the free daughters (22). The extent to which such interventions are needed will likely depend on the residence time of the antibody in circulation and the internalization properties of the antibody-antigen complex. In a recent update of results from a clinical trial of ^{225}Ac-HuM195 antibody in leukemia patients, no acute toxicity was seen and no evidence of radiation nephritis has been seen, with follow-up to 10 months in patients receiving up to 4 μCi/kg (28). Liposomal encapsulation of ^{225}Ac (29) has also been proposed to trap free ^{225}Ac daughters. Extracorporeal metal chelation of blood ^{221}Fr and ^{213}Bi could also be used to reduce renal toxicity (30). Interestingly, ^{225}Ac-labeled anti-thrombomodulin mAb (201B, targeting lung vasculature) caused lethal toxicity to the lungs, whereas it was able to inhibit metastatic growth (31). No evident damage to lung tissue was observed when rat HER-2/*neu* was targeted in this study, showing the importance of selecting tumor antigen for targeting to reduce toxicity.

The reduced efficacy when treating micrometastases at 18 day after cancer cell inoculation was expected and may be partially explained by increased tumor burden and increased tumor heterogeneity leading to nonuniform dose distributions (32). Monte Carlo modeling has shown that, when treating a micrometastases containing 1,000 cancer cells, the tumor control probability could drop from 93% to 0% when a 50% variance of antigen expression was introduced to a uniform expression (33). A recent clinical trial has shown that consolidation of chemotherapy regimen with ^{213}Bi-HuM195 in acute myeloid leukemia patients is highly effective (34). The efficacy data from days 18 and 3 metastatic models suggest that ^{225}Ac-based radioimmunotherapy should be tested ideally in patients undergoing remission after first line chemotherapy treatments.

In conclusion, we have shown that α-particle emitter ^{225}Ac-labeled mAb is very effective, better than the α-emitter, ^{213}Bi, and the β-emitter, ^{90}Y, in prolonging the survival of *neu*-N transgenic mice bearing lung metastases. Long-term renal toxicity was observed and approaches designed to mitigate such toxicity (22) may need to be implemented in clinical studies.

Disclosure of Potential Conflicts of Interest

No potential conflicts of interest were disclosed.

Acknowledgments

Received 5/20/09; revised 9/3/09; accepted 9/17/09; published OnlineFirst 11/17/09.

Grant support: National Cancer Institute grant R01 CA 113797 and Department of Defense Fellowship BC0444176 to H. Song.

The costs of publication of this article were defrayed in part by the payment of page charges. This article must therefore be hereby marked *advertisement* in accordance with 18 U.S.C. Section 1734 solely to indicate this fact.

References

1. McDevitt MR, Sgouros G, Finn RD, et al. Radioimmunotherapy with α-emitting nuclides. Eur J Nucl Med 1998;25:1341–51.
2. Nikula TK, McDevitt MR, Finn RD, et al. α-Emitting bismuth cyclohexylbenzyl DTPA constructs of recombinant humanized anti-CD33 antibodies: pharmacokinetics, bioactivity, toxicity and chemistry. J Nucl Med 1999; 40:166–76.
3. McDevitt MR, Barendswaard E, Ma D, et al. An α-particle emitting bismuth-213 labeled antibody (J591) to the external domain of prostate specific membrane antigen. Cancer Res 2000;60:6095–100.
4. Song EY, Qu CF, Rizvi SMA, et al. Bismuth-213 radioimmunotherapy with C595 anti-MUC1 monoclonal antibody in an ovarian cancer ascites model. Cancer Biol Ther 2008;7:76–80.
5. Milenic DE, Garmestani K, Brady ED, et al. Targeting of HER2 antigen for the treatment of disseminated peritoneal disease. Clin Cancer Res 2004;10:7834–41.
6. Song H, Shahverdi K, Huso DL, et al. Bi-213 (α-emitter)-antibody targeting of breast cancer metastases in the neu-N transgenic mouse model. Cancer Res 2008;68:3873–80.
7. Jurcic JG, Caron PC, Nikula TK, et al. Radiolabeled anti-CD33 monoclonal antibody M195 for myeloid leukemias. Cancer Res 1995;55:5908–10s.
8. Jurcic JG, Larson SM, Sgouros G, et al. Targeted alpha-particle immunotherapy for myeloid leukemia. Blood 2002;100:1233–9.
9. McDevitt MR, Ma D, Lai LT, et al. Tumor therapy with targeted atomic nanogenerators. Science 2001;294:1537–40.
10. Borchardt PE, Yuan RR, Miederer M, McDevitt MR, Scheinberg DA. Targeted actinium-225 *in vivo* generators for therapy of ovarian cancer. Cancer Res 2003;63:5084–90.
11. Singh JJ, Henke E, Seshan SV, et al. Selective α-particle mediated depletion of tumor vasculature with vascular normalization. PLoS ONE 2007;2:e267.
12. Milenic DE, Garmestani K, Brady ED, et al. Potentiation of high-LET radiation by gemcitabine: targeting HER2 with trastuzumab to treat disseminated peritoneal disease. Clin Cancer Res 2007;13:1926–35.
13. Dahle J, Borrebaek J, Jonasdottir TJ, et al. Targeted cancer therapy with a novel low-dose rate α-emitting radioimmunoconjugate. Blood 2007;110:2049–56.
14. Behr TM, Behe M, Stabin MG, et al. High-linear energy transfer (LET) α versus low-LET β emitters in radioimmunotherapy of solid tumors: therapeutic efficacy and dose-limiting toxicity of 213Bi- versus 90Y-labeled CO17-1A Fab′ fragments in a human colonic cancer model. Cancer Res 1999;59:2635–43.
15. Slamon DJ, Clark GM, Wong SG, Levin WJ, Ullrich A, Mcguire WL. Human-breast cancer—correlation of relapse and survival with amplification of the Her-2 neu oncogene. Science 1987;235:177–82.
16. Piccart-Gebhart MJ, Procter M, Leyland-Jones B, et al. Trastuzumab after adjuvant chemotherapy in HER2-positive breast cancer. N Engl J Med 2005;353:1659–72.
17. Song H, Shahverdi K, Huso DL, et al. An immunotolerant HER-2/neu transgenic mouse model of metastatic breast cancer. Clin Cancer Res 2008;14:6116–24.
18. Reilly RT, Gottlieb MBC, Ercolini AM, et al. HER-2/neu is a tumor rejection target in tolerized HER-2/neu transgenic mice. Cancer Res 2000;60:3569–76.
19. Brechbiel MW, Pippin CG, Mcmurry TJ, et al. An effective chelating agent for labeling of monoclonal-antibody with Bi-212 for α-particle mediated radioimmunotherapy. J Chem Soc Chem Commun 1991;1169–70.

Published OnlineFirst November 17, 2009; DOI: 10.1158/0008-5472.CAN-09-1828

20. McDevitt MR, Ma D, Simon J, Frank RK, Scheinberg DA. Design and synthesis of 225Ac radioimmunopharmaceuticals. Appl Radiat Isot 2002;57:841–7.

21. Carrasquillo JA, White JD, Paik CH, et al. Similarities and differences in In-111- and Y-90-labeled 1B4M-DTPA antiTac monoclonal antibody distribution. J Nucl Med 1999;40:268–76.

22. Jaggi JS, Kappel BJ, McDevitt MR, et al. Efforts to control the errant products of a targeted *in vivo* generator. Cancer Res 2005;65:4888–95.

23. Song H, Du Y, Sgouros G. Therapeutic potential of Y-90- and I-131-labeled anti-CD20 monoclonal antibody in treating non-Hodgkin's lymphoma with pulmonary involvement: a Monte Carlo-based dosimetric analysis. J Nucl Med 2007;48:150–7.

24. Hamacher KA, Den RB, Den EI, Sgouros G. Cellular dose conversion factors for α-particle-emitting radionuclides of interest in radionuclide therapy. J Nucl Med 2001;42:1216–21.

25. Goddu SM, Howell RL, Bouchet LG, Bolch WE, Rao DV. MIRD cellular S values. Reston (VA): Society of Nuclear Medicine; 1997.

26. Stein R, Govindan SV, Chen S, et al. Radioimmunotherapy of a human lung cancer xenograft with monoclonal antibody RS7: evaluation of Lu-177 and comparison of its efficacy with that of Y-90 and residualizing I-131. J Nucl Med 2001;42:967–74.

27. Miederer M, McDevitt MR, Sgouros G, Kramer K, Cheung NK, Scheinberg DA. Pharmacokinetics, dosimetry, and toxicity of the targetable atomic generator, 225Ac-HuM195, in nonhuman primates. J Nucl Med 2004;45:129–37.

28. Scheinberg DA, McDevitt MR, Larson SM, Jurcic JG, Villa C, EScorcia F. α-Particle Immunotherapy with Bi-213 and Ac-225-antibodies. 2009.

29. Sofou S, Thomas JL, McDevitt MR, Scheinberg DA, Sgouros G. Engineered liposomes for potential α-particle therapy of metastatic cancer. J Nucl Med 2004; 45:253–60.

30. Wang Z, Garkavij M, Tennvall JG, Ohlsson T, Strand SE, Sjogren HO. Application of extracorporeal immunoadsorption to reduce circulating blood radioactivity after intraperitoneal administration of indium-111-HMFG1-biotin. Cancer 2002;94:1287–92.

31. Kennel SJ, Chappell LL, Dadachova K, et al. Evaluation of 225Ac for vascular targeted radioimmunotherapy of lung tumors. Cancer Biother Radiopharm 2000;15:235–44.

32. Braun S, Hepp F, Sommer HL, Pantel K. Tumor-antigen heterogeneity of disseminated breast cancer cells: implications for immunotherapy of minimal residual disease. Int J Cancer 1999;84:1–5.

33. Sgouros G, Song H. Cancer stem cell targeting using the α-particle emitter, Bi-213: mathematical modeling and feasibility analysis. Cancer Biother Radiopharm 2008;23:74–81.

34. Rosenblat T, McDevitt MR, Mulford DA, et al. Sequential cytarabine and α-particle immunotherapy with bismuth-213 (Bi-213)-labeled-HuM195 (lintuzumab) for acute myeloid leukemia (AML). Blood 2008; 112:1025.

Cancer Research
The Journal of Cancer Research (1916–1930) | The American Journal of Cancer (1931–1940)

AACR American Association for Cancer Research

Radioimmunotherapy of Breast Cancer Metastases with α -Particle Emitter ^{225}Ac: Comparing Efficacy with ^{213}Bi and ^{90}Y

Hong Song, Robert F. Hobbs, Ravy Vajravelu, et al.

Cancer Res 2009;69:8941-8948. Published OnlineFirst November 17, 2009.